

## Structural properties of ZnO nanopowders synthesized by thermal decomposition

Y.Y. Kedruk , Zh.U. Paltusheva , L.V. Gritsenko\*  and V. Syritski 

<sup>1</sup>Kazakh-British Technical University, Almaty, Kazakhstan

<sup>2</sup>Satbayev University, Almaty, Kazakhstan

<sup>3</sup>Department of Materials and Environmental Technology, Tallinn University of Technology, Tallinn, Estonia

\*e-mail: [l.gritsenko@satbayev.university](mailto:l.gritsenko@satbayev.university)

(Received September 28, 2023; received in revised form October 27, 2023; accepted November 8, 2023)

Zinc oxide nanostructures attract considerable attention of researchers due to their unique properties such as electrical conductivity, piezoelectric properties, optical transparency, emission, wide forbidden zone. Zinc oxide nanopowders are obtained by various methods: hydrothermal synthesis, sol-gel method, pyrolysis, chemical precipitation from solution and others. The task of development of low-cost methods of zinc oxide synthesis with high reproducibility is actual. The thermal decomposition method is a controlled relatively inexpensive method that can enable large scale production without the use of complex equipment and expensive materials. In this work, nanostructured ZnO samples were prepared by thermal decomposition of zinc acetate dehydrate at temperatures 400 °C and 700 °C. The influence of such synthesis parameters as duration and temperature on the morphology and structural properties of the obtained samples were investigated. It was found that the morphology of the synthesised ZnO samples significantly depends on the synthesis temperature. The obtained Raman scattering spectra show characteristic peaks of zinc oxide and carbon. An efficient, inexpensive method for the synthesis of zinc oxide nanoparticles with controlled morphology, promising for use as photocatalysts, the basis for the development of sensor devices, is presented.

**Key words:** thermal decomposition, zinc oxide, nanopowders, structural properties, raman spectra.

**PACS number(s):** 78.67.Bf, 87.64.-t, 81.10.Dn, 78.55.Et.

### 1 Introduction

The development and investigation of properties of nanocrystalline materials is an important and urgent task. Metal-oxide nanostructures are promising materials for applications in various fields of chemistry, materials science, physics and biotechnology due to their unique electronic structure [1, 2]. Transition metal ions usually possess unfilled d-shells, which provides reactive electronic transitions, wide bandgap, excellent electrical characteristics and high dielectric constant [3]. Metal-oxide nanomaterials possess exceptional and tunable optoelectronic, optical, electrical, thermal, magnetic, catalytic, mechanical, and photochemical properties, enabling them to be used with high efficiency to produce sensors [4, 5], fuel cells, batteries, supercapacitors, and optical devices [6]. The above wide range of applications is also due to the high surface density of these nanostructures [7].

Zinc oxide, due to its wide bandgap (3.3 eV at room temperature), large exciton binding energy (60 meV) and high melting temperature (2248 K) is one of the promising semiconductors [8]. ZnO nanomaterials, compared to bulk ZnO analogues, demonstrate new properties that are applicable for the development of biosensors, ultraviolet lasers, frequency converters, nanoscale optical circuits, etc. [9-11]. The activity of the obtained ZnO nanomaterials depends on their physicochemical properties such as shape, size, surface area, and crystal structure. The need to synthesise low-dimensional structures with certain characteristics has led to the development of a wide variety of methods for the synthesis of zinc oxide [12, 13]. ZnO nanoparticles can be produced on a large scale by simple synthesis methods such as chemical precipitation [14], sol-gel method [15], solvothermal/hydrothermal synthesis methods [16, 17] and others.

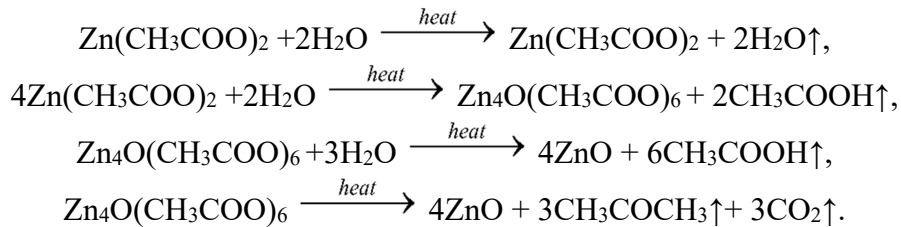
Among various methods of ZnO synthesis, thermal decomposition is a relatively inexpensive

method that does not require expensive raw materials and complex equipment. Studies [18-20] confirm that the synthesis of nanoparticles by this method proceeds without organic and toxic solvents, and the obtained zinc oxide samples have high activity and high specific surface area. Depending on the synthesis parameters, ZnO particles of various sizes and morphologies are formed [21]. Studies [22-24] have shown a strong dependence of microstructure and physical properties of synthesised ZnO samples on the synthesis temperature.

In the presented work, the influence of factors such as temperature and synthesis time on the structural properties and morphology of the synthesised samples has been studied.

## 2 Description of the experiment and discussion of the results

The synthesis of ZnO NPs nanoparticles was carried out by thermal decomposition of zinc acetate dihydrate  $(\text{CH}_3\text{COO})_2\text{Zn}\cdot 2\text{H}_2\text{O}$  in a muffle furnace in atmosphere at temperatures of 400°C and 700°C, the duration of annealing was 2, 4, 6 and 10 hours. Zinc acetate was placed in a ceramic crucible covered with a ceramic lid. The mass of the obtained ZnO NPs sample was (1/4 – 1/3) of the mass of zinc acetate. According to [25], the main weight loss is due to the evaporation of acetone  $((\text{CH}_3)_2\text{CO})$  and carbon dioxide  $(\text{CO}_2)$  in the precursor. The process occurring during the formation of ZnO can be explained by the following reactions [25]:



By this method samples at 400°C: #1 (annealing duration 2 hours), #2 (annealing duration 4 hours), #3 (annealing duration 6 hours), #4 (annealing duration 10 hours), at 700°C: #5 (annealing duration 2 hours), #6 (annealing duration 4 hours), #7 (annealing duration 6 hours), #8 (annealing duration 10 hours) were synthesised.

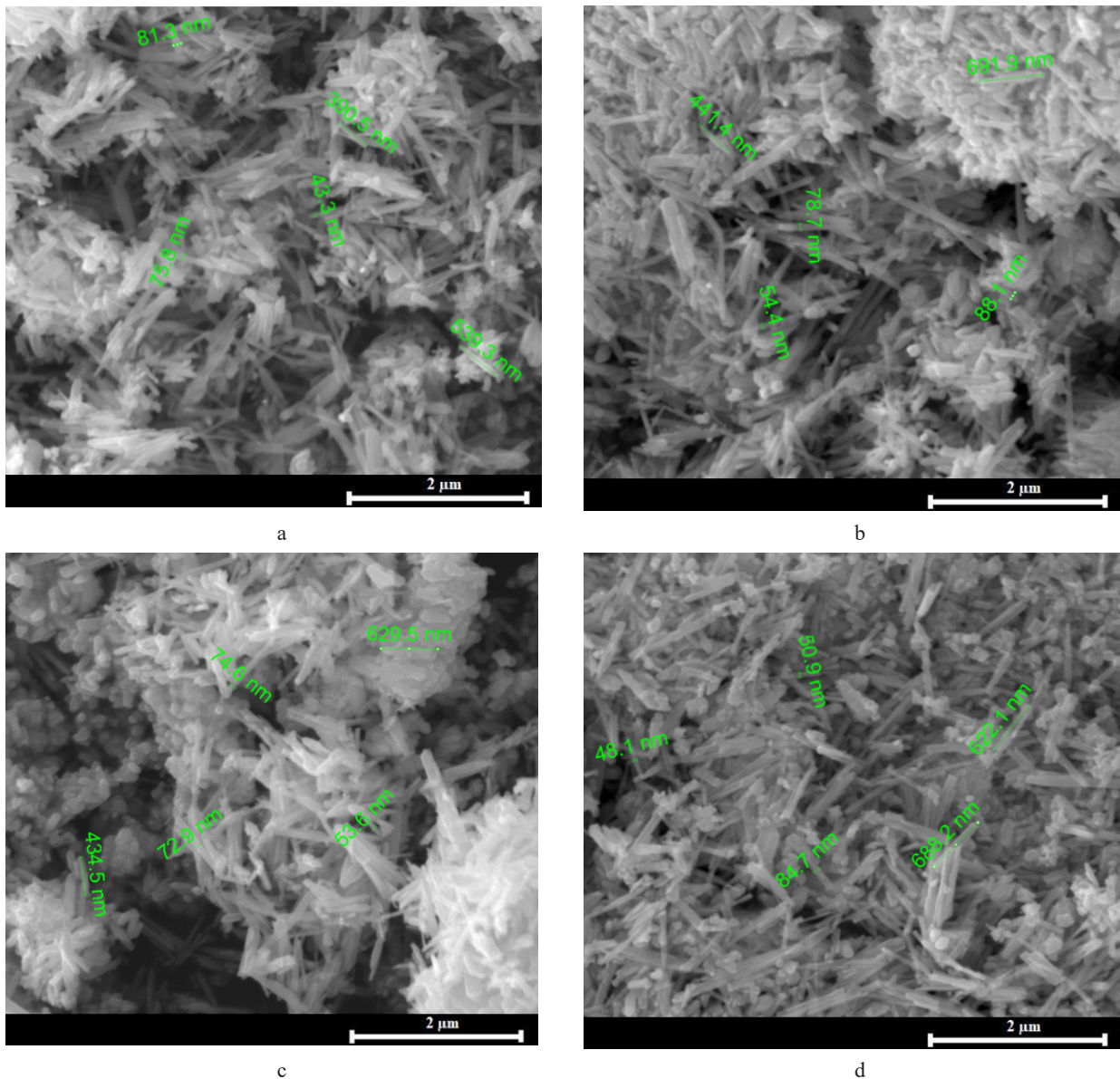
The prepared ZnO samples were investigated by scanning electron microscopy. Figures 1, 2 and

Table 1 show the results of SEM morphology of ZnO powders synthesised by thermal decomposition of zinc acetate.

Samples #1, #2, #3 and #4 are samples synthesized by thermal decomposition of zinc acetate in an atmosphere at 400°C for two, four, six and ten hours, respectively. Samples #5, #6, #7 and #8 were synthesized at 700°C for two, four, six and ten hours, respectively.

**Table 1** – Physicochemical properties of ZnO nanoparticles.

Sample	SEM		Aspect Ratio (AR), l/d	Cell parameters, Å	
	Thickness d, nm	Length l, nm		a	c
#1	55±20	450±50	8.2	3.255	5.214
#2	65±20	580±50	8.9	3.252	5.210
#3	67±20	625±50	9.3	3.246	5.201
#4	68±20	650±50	9.6	3.245	5.200
#5	105±20	250±50	2.4	3.253	5.212
#6	125±20	350±50	2.8	3.253	5.211
#7	130±20	635±50	4.9	3.247	5.203
#8	150±20	780±50	5.2	3.243	5.197



**Figure 1** – SEM of ZnO samples synthesized by thermal decomposition of zinc acetate in an atmosphere at 400°C: (a) #1, (b) #2, (c) #3 and (d) #4

The electron microscopy study showed that annealing at 400°C produces thinner long ZnO rods (Figure 1). At annealing of zinc acetate at 700°C oblong ZnO particles are formed, geometrical parameters of which slightly increase at longer annealing of ZnAc<sub>2</sub> (Figure 2).

Figure 3 shows the results of the synthesised nanoparticles as well as the plant sample of ZnO by XRD analysis. XRD measurements were performed under the same conditions for all samples. All investigated ZnO samples show hexagonal wurtzite

structure. ZnO samples obtained by thermal annealing of zinc acetate in air have a structure close to the reference sample (JCPDS map No. 70-8072) with lattice parameters  $a = 3.2465 \text{ \AA}$  and  $c = 5.2030 \text{ \AA}$ . It was observed that the [100], [101] and [002] reflexes had the highest intensity, with the intensity of the reflexes increasing with increasing annealing duration. Among all the diffraction peaks, the intense reflex (101) (Figure 3) stands out especially, demonstrating the crystalline nature of ZnO nanoparticles.

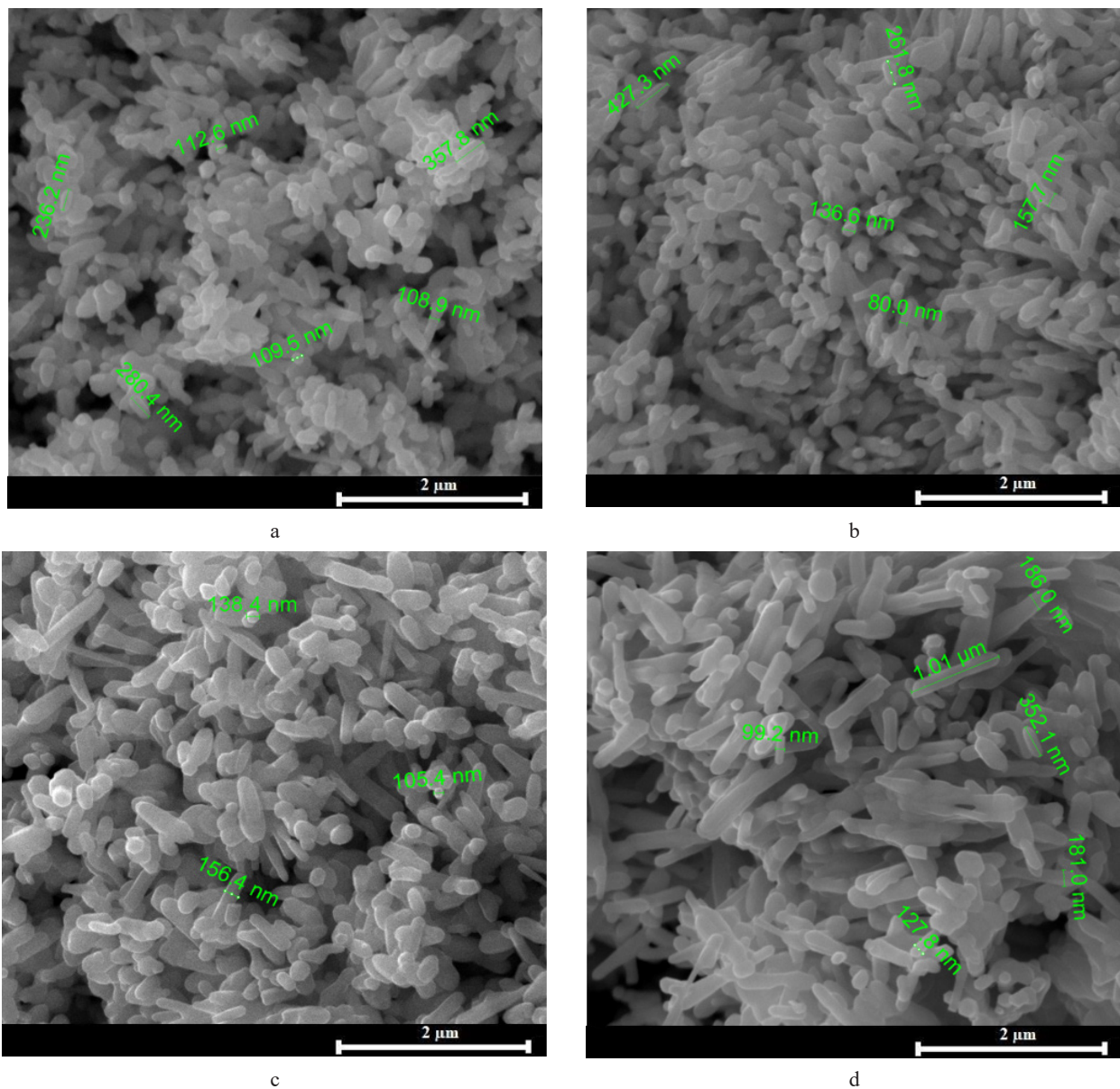


**Figure 2** – SEM of ZnO samples synthesized by thermal decomposition of zinc acetate in an atmosphere at 700°C: (a) #5, (b) #6, (c) #7 and (d) #8

The synthesized samples #1 – #8 were also studied by Raman spectroscopy. Raman spectra of the samples obtained by annealing zinc acetate at 400°C are shown in Figure 4, where the bands of vibrational modes are observed: D at  $\sim 1379\text{ cm}^{-1}$  and G at  $\sim 1584\text{ cm}^{-1}$ , characteristic of the structure of nanocrystalline graphite, as well as modes  $\sim 99\text{ cm}^{-1}$  and  $\sim 438\text{ cm}^{-1}$ , which correspond to the peaks of zinc oxide. Increasing the annealing time of zinc acetate

promotes the appearance of the ZnO mode  $\sim 438\text{ cm}^{-1}$ , which indicates the crystallisation of the samples.

The analysis of Raman spectra of the studied ZnO samples showed that at the annealing temperature of 400°C there are ZnO peaks and amorphous carbon phase. It was noted that the increase of annealing duration and temperature increase up to 700°C favours the increase of Raman signal, formation and improvement of ZnO crystal structure.

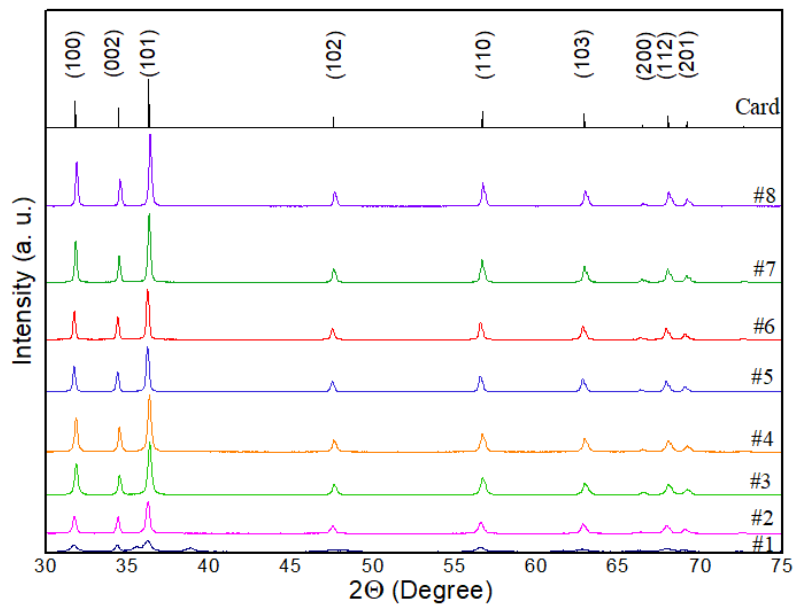


Figure 3 – X-ray diffraction patterns of ZnO samples obtained by annealing zinc acetate in atmosphere

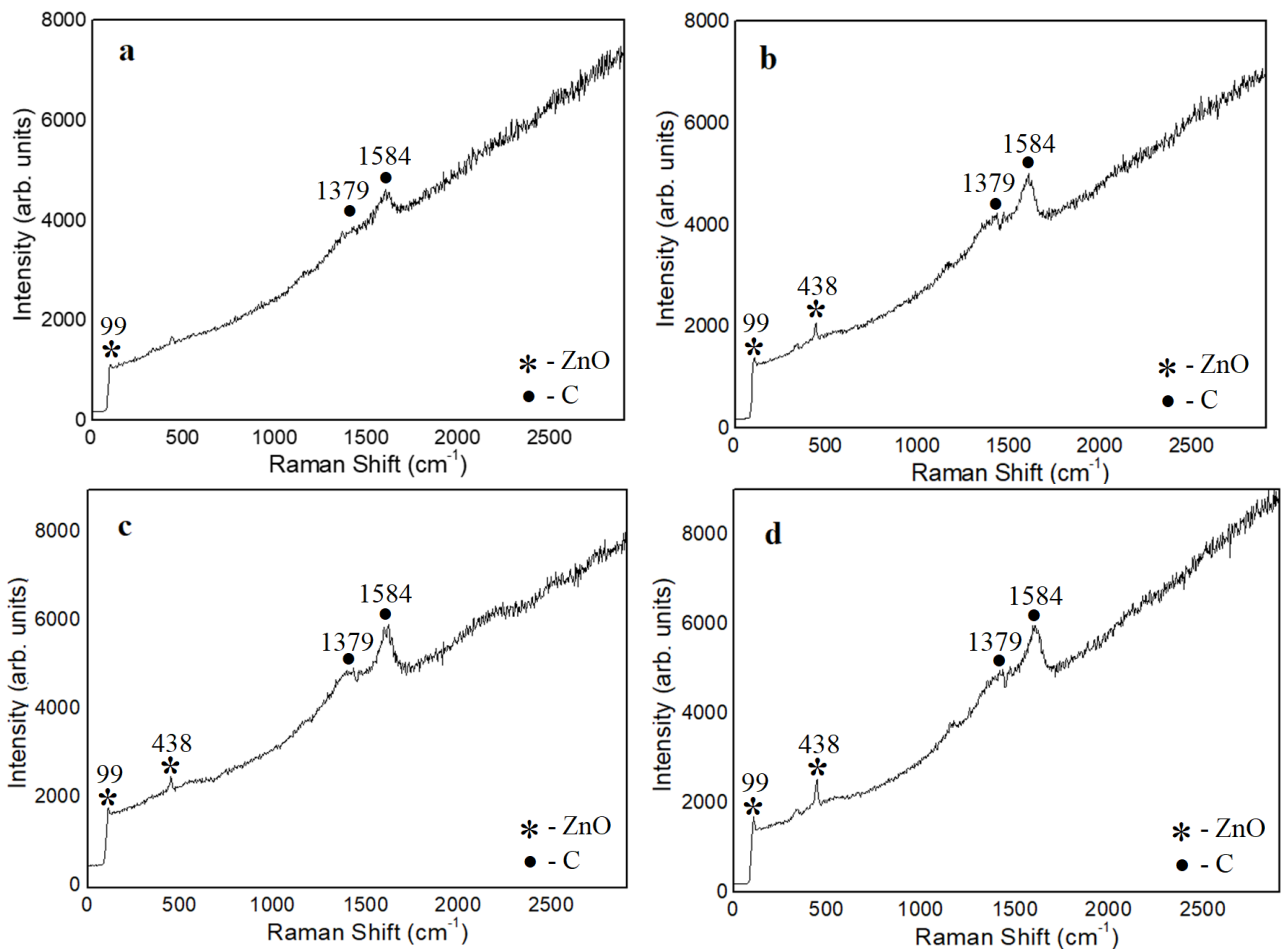
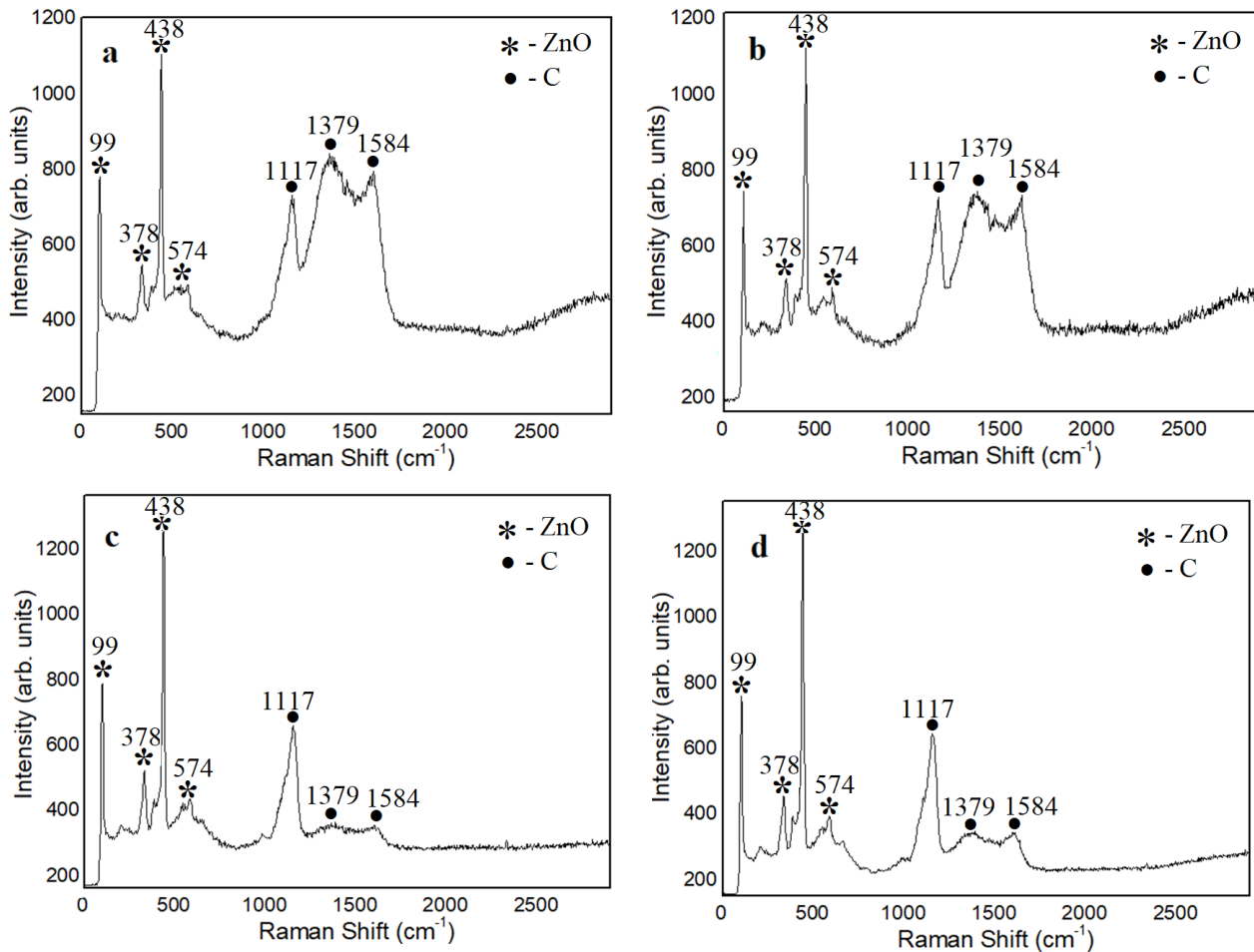


Figure 4 – Raman spectra of ZnO samples obtained by thermal decomposition of zinc acetate in an atmosphere at 400°C: (a) #1, (b) #2, (c) #3 and (d) #4



**Figure 5** – Raman spectra of ZnO samples obtained by thermal decomposition of zinc acetate in an atmosphere at 700°C: (a) #5, (b) #6, (c) #7 and (d) #8

Figure 5 shows that upon annealing zinc acetate at 700°C, the following modes are observed:  $\sim 99$   $\text{cm}^{-1}$ ,  $378$   $\text{cm}^{-1}$ ,  $438$   $\text{cm}^{-1}$ ,  $574$   $\text{cm}^{-1}$ , corresponding to zinc oxide nanocrystals with wurtzite structure. The narrow band at  $438$   $\text{cm}^{-1}$  indicates good crystallinity of the ZnO samples, while the relatively narrow mode band at  $378$   $\text{cm}^{-1}$  indicates particle ordering. The energies of phonon scattering active in ZnO samples are in satisfactory agreement with the known data for ZnO crystals.

The spectrum in Figure 5 also shows bands at  $1117$   $\text{cm}^{-1}$ ,  $1376$   $\text{cm}^{-1}$  and  $1588$   $\text{cm}^{-1}$ , characteristic of amorphous carbon films. With increasing annealing time, the intensity of the peaks of amorphous silicon decreases, while the intensity of the vibrational modes of crystalline ZnO increases.

## Conclusions

ZnO nanoparticles with different morphology were synthesized by thermal decomposition method. It is shown that all samples absorb light in the UV range. It is shown that the obtained ZnO samples have a structure close to the reference sample (JCPDS map No. 70-8072) with lattice parameters  $a - 3.2465$  Å and  $c - 5.2030$  Å. Among all the diffraction peaks, an intense reflex (101) is particularly prominent, demonstrating the crystalline nature of ZnO nanoparticles. The analysis of Raman spectra of the investigated ZnO samples showed that increasing the annealing duration and increasing the temperature up to  $700$  °C favours the increase of Raman signal, formation and improvement of the crystal structure of ZnO.

## References

1. Fikadu T. G., Mesfin A. K., Megersa W. S., Fekadu G. H. Experimental and computational study of metal oxide nanoparticles for the photocatalytic degradation of organic pollutants: a review // *RSC Advances*. – 2023. – Vol. 13 (27). – P.18404-18442. <https://doi.org/10.1039/D3RA01505J>
2. Shabdan Y., Markhabayeva A., Bakranov N., Nuraje N. Photoactive Tungsten-Oxide Nanomaterials for Water-Splitting // *Nanomaterials*. – 2020. – Vol. 10. – P. 1871. <https://doi.org/10.3390/nano10091871>
3. Yeosang Y., Phuoc L. T., Daeho L., Seung H. K. Metal-Oxide Nanomaterials Synthesis and Applications in Flexible and Wearable Sensors // *ACS Nanosci. Au*. – 2022. – Vol. 2 (2). – P. 64–92. <https://doi.org/10.1021/acsnanoscienceau.1c00029>
4. Paltusheva Z.U., Ashikbayeva Z., Tosi D., Gritsenko L.V. Highly Sensitive Zinc Oxide Fiber-Optic Biosensor for the Detection of CD44 Protein // *Biosensors*. – 2022. – Vol. 12. – P. 1015. <https://doi.org/10.3390/bios12111015>
5. Bakranova D., Seitov B., Bakranov N. Photocatalytic and Glucose Sensing Properties of ZnO-Based Nanocoating // *ChemEngineering*. – 2023. – Vol. 7. – P. 22. <https://doi.org/10.3390/chemengineering7020022>
6. Alhalili Z. Metal Oxides Nanoparticles: General Structural Description, Chemical, Physical, and Biological Synthesis Methods, Role in Pesticides and Heavy Metal Removal through Wastewater Treatment // *Molecules*. – 2023. – Vol. 28. – P. 3086. <https://doi.org/10.3390/molecules28073086>
7. Negrescu A.M., Killian M.S., Raghu S.N.V., Schmuki P., Mazare A., Cimpean A. Metal Oxide Nanoparticles: Review of Synthesis, Characterization and Biological Effects // *J. Funct. Biomater*. – 2022. – Vol. 13. – P. 274. <https://doi.org/10.3390/jfb13040274>
8. Raha S. and Md. Ahmaruzzaman. ZnO nanostructured materials and their potential applications: progress, challenges and perspectives // *Nanoscale Adv.* – 2022. – V. 4. – 1868-1925. <https://doi.org/10.1039/D1NA00880C>
9. Sharma D. K., Shukla S., Sharma K. K., Kumar V. A review on ZnO: Fundamental properties and applications // *Materials Today: Proceedings*. – 2020. – V. 49. – P.3028-3035. <https://doi.org/10.1016/j.matpr.2020.10.238>
10. Sulciute A., Nishimura K., Gilshtein E., Cesano F., Viscardi G., Nasibulin A. G., Ohno Y., Rackauskas S. ZnO Nanostructures Application in Electrochemistry: Influence of Morphology // *J. Phys. Chem.* – 2021. – V. 125 (2). – P. 1472–1482. <https://doi.org/10.1021/acs.jpcc.0c08459>
11. Tolubayeva D.B., Gritsenko L.V., Kedruk Y.Y., Aitzhanov M.B., Nemkayeva R.R., Abdullin K.A. Effect of Hydrogen Plasma Treatment on the Sensitivity of ZnO Based Electrochemical Non-Enzymatic Biosensor // *Biosensors*. – 2023. – Vol. 13. – P. 793. <https://doi.org/10.3390/bios13080793>
12. Ravi R., Netram K. The structural and optical properties of ZnO nanoparticles synthesized via thermal decomposition // *Materials Today: Proceedings*. – 2022. – Vol. 54 (3). – P. 624-627. <https://doi.org/10.1016/j.matpr.2021.10.207>
13. Kh. A. Abdullin, M. T. Gabdullin, L.V. Gritsenko, D.V. Ismailov, Zh. K. Kalkozova, S.E. Kumekov, Zh. O. Mukash, A. Yu Sazonov, E.I. Terukov. Electrical, optical, and photoluminescence properties of ZnO films subjected to thermal annealing and treatment in hydrogen plasma // *Semiconductors*. – 2016. – Vol. 50 (8). – P.1010–1014. <https://doi.org/10.1134/S1063782616080029>
14. Taka G., Das T. D. Synthesis of ZnO nanoparticles through a simple wet chemical precipitation method // *IOP Conf. Series: Earth and Environmental Science*. – 2022. – Vol.1042. – P. 1-6. <http://dx.doi.org/10.13005/ojc/310281>
15. Ben Amor I., Hemmami H., Laouini S.E., Mahboub, M.S., Barhoum A. Sol-Gel Synthesis of ZnO Nanoparticles Using Different Chitosan Sources: Effects on Antibacterial Activity and Photocatalytic Degradation of AZO Dye // *Catalysts*. – 2022. – Vol. 12. – P. 1611. <https://doi.org/10.3390/catal12121611>
16. Šarić A., Despotović I., Štefanić G. Solvothermal synthesis of zinc oxide nanoparticles: A combined experimental and theoretical study // *Journal of Molecular Structure*. – 2019. – Vol.15. – P. 251-260. <https://doi.org/10.1016/j.molstruc.2018.10.025>
17. Kh.A. Abdullin, M.T. Gabdullin, S.K. Zhumagulov, G.A. Ismailova, L.V. Gritsenko, Y.Y. Kedruk, M. Mirzaeian. Stabilization of the surface of ZnO films and elimination of the aging effect // *Materials*. – 2021. – Vol. 14 (21). – P. 6535. <https://doi.org/10.3390/ma14216535>
18. Wisetrinthong C., Pinitsoontorn S., Kidkhunthod P., Wongsaprom K. Thermal decomposition synthesis and magnetic properties of crystalline zinc oxide powders // *Journal of Physics: Conference Series*. – 2018. – Vol. 1144. – P.012078. <https://doi.org/10.1088/1742-6596/1144/1/012078>
19. Radovanović L., Zdravković J. D., Simović B., Radovanović Ž., Mihajlovski K., Dramićanin M. D., Rogan J. Zinc oxide nanoparticles prepared by thermal decomposition of zinc benzenepolycarboxylato precursors: Photoluminescent, photocatalytic and antimicrobial properties // *J. Serb. Chem. Soc.* – 2020. – Vol. 85 (11). – P. 1475 – 1488. <https://doi.org/10.2298/JSC200629048R>
20. Kedruk Y.Y., Baigarinova G.A., Gritsenko L.V., Cicero G., Abdullin K.A. Facile Low-Cost Synthesis of Highly Photocatalytically Active Zinc Oxide Powders // *Front. Mater.* – 2022. – Vol. 9. – P. 869493. <https://doi.org/10.3389/fmats.2022.869493>
21. Svetozar M., Ankica Š., Stanko P. Formation of nanosize ZnO particles by thermal decomposition of zinc acetylacetonate monohydrate // *Ceramics International*. – 2010. – Vol. 36 (3). – P. 1117-1123. <https://doi.org/10.1016/j.ceramint.2009.12.008>
22. Wisetrinthong C., Pinitsoontorn S., Kidkhunthod P., Kwanruthai W. Thermal decomposition synthesis and magnetic properties of crystalline zinc oxide powders // *J. Phys.: Conf. Ser.* – 2018. Vol. 1144 (1). – P. 012078. <https://doi.org/10.1088/1742-6596/1144/1/012078>
23. Armah N. A. A., Koffi H. A. Temperature Dependence on Structural Properties of Liquid Phase Synthesized ZnO // *Adv. Nan. Res.* – 2023. – Vol. 6 (1). – P. 11–28. <https://doi.org/10.21467/anr.6.1.11-28>
24. Kasahun M., Yadate A., Belay A., Belay Z., Ramalingam M. Antimicrobial Activity of Chemical, Thermal and Green Route-Derived Zinc Oxide Nanoparticles: A Comparative Analysis // *Nano Biomed. Eng.* – 2020. – Vol. 12(1). – P. 47-56. <https://doi.org/10.5101/nbe.v12i1.p47-56>
25. Zakria M., Huynh T. T., Ling F. C. C., Su S. C., Phillips M. R., Ton-That C. Highly Luminescent MgZnO/ZnO Multiple Quantum Wells for Photonics Devices // *ACS Appl. Nano Mater.* – 2019. – Vol. 2 (4). – P. 2574–2579. <https://doi.org/10.1021/acsanm.9b00592>